Tracing of Uranium isotopes and man-made radionuclides in contaminated soils at the nuclear testing site at Maralinga, SA

Thesis submitted in accordance with the requirements of the University of Adelaide for an Honours Degree in Environmental Geoscience

Jason Charlwood

November 2022

THE UNIVERSITY of ADELAIDE

ABSTRACT

Various nuclear fission and explosion trials were held at Maralinga, South Australia by the United Kingdom from 1956 to 1963. Seven large trials each using atomic bombs of varying designs were detonated over this period. In addition to the seven large scale trials, numerous minor trials were also performed within this period, and these are reported to have caused the greatest environmental impact to the area, via dispersal of plutonium and uranium and related radionuclides. Fissile material used in the atomic weapons tested at Maralinga generally comprised ^{235}U. Residual contamination is still present today in local soils; Although at greatly reduced levels it still poses a potential risk to humans through ingestion of airborne 'hot' particles which have a bulk composition of plutonium and uranium oxide. Enrichment of ^{235}U in soils may therefore infer distribution of residual radionuclide contamination associated with historical atomic weapons testing. This research seeks to use the $^{235}U/^{238}U$ isotopic ratio obtained from Maralinga soil as well as control samples from various natural sources, to generate a method that can constrain the limits of man-made nuclear contamination across Maralinga sites. Gamma spectroscopy was used to identify both natural and man-made radionuclides in samples. Analysis of bulk soils collected from across Maralinga test sites did not find a ^{235}U enrichment within a 0.14% error margin (relative to the abundance of ^{238}U), obtained through analytical uncertainty of uranium isotope measurements. The $^{235}U/^{238}U$ ratios of Maralinga soils and uncontaminated soils all presented a quasi-natural isotope ratio near the proposed value of natural uranium standard CRM 145 of 0.00725. However, gamma spectroscopy data shows that the Maralinga soils still contain an excess of various man-made radionuclides indicative of nuclear fission waste products such as ^{241}Am, ^{137}Cs and ^{152}Eu. Neither induction coupled plasma mass spectrometry or gamma spectroscopy analytical approaches used in this study were suitable for the detection of ^{239}Pu. Overall, we conclude that ^{235}U present from nuclear testing may be present at concentrations but do not significantly influence or vary from the 'natural' or background $^{235}U/^{238}U$ isotope composition. The uranium isotope ratio does not appear to be a beneficial marker of residual radionuclide distribution in the Maralinga area based on the limited number of samples assessed. Gamma spectroscopy assessment of collected soils infers radionuclide distribution is not homogeneous across the Maralinga area, Further assessment using a grid sampling approach would provide better resolution of radionuclide distribution across the Maralinga area.

KEYWORDS

Soil Contamination; Environmental Impact; Hot particles; Maralinga; Nuclear testing; Radionuclides; Uranium isotopes, 'Hot' Particles

CONTENTS

LIST OF FIGURES AND TABLES

ACRONYMS AND ABBREVIATIONS

CRREI	Centre for Radiation Research Education and Innovation
EDS	Energy dispersive Spectroscopy
HF	Hydrofluoric acid
HPGe	high purity germanium
HNO_3	Nitric acid
ICP-MS	Induction coupled plasma mass spectrometry
MDA	Minimum detectable activity
SA EPA	South Australian Environment Protection Authority
SEM	Scanning Electron microscope
SSB	Sample-Standard Bracketing
TAG	Technical Assessment Group
UKAWRE	United Kingdom Atomic Weapons Research Establishment
GS	Gamma spectroscopy
HPULBLS	high performance ultra-low background lead shield

SITE ABBREIVATIONS

B	Breakaway (Maralinga)
CP	Coober Pedy (South Australia)
OT	One Tree (Maralinga)
T	Tadje (Maralinga)
TA	Taranaki (Maralinga)
UITE	Uraninite (Bohemia)

1. INTRODUCTION

The United Kingdom Atomic Weapons Research Establishment (UKAWRE) undertook numerous atomic weapons trials at Maralinga, South Australia (SA) with the first detonation occurring in 1956 and ceasing in 1963. Maralinga, with its history and the legacy of former nuclear testing serves as a unique example of such significant contamination by a variety of man-made radionuclides distributed over a vast area, covering ca. 52,000 km^2 area (Lorna Arnold, 2006). Consequentially, between 1952 and 1981 the traditional owners of the Maralinga-Emu lands were denied access to their lands. In 2009, the Maralinga Tjarutja people officially had their land returned to them. This full return of land was planned to occur in 1984, but two sites were withheld due to potentially high radionuclide contamination still present (MRTAC, 2003).

The tests conducted at Maralinga served to develop various aspects of nuclear weapons with 4 major trials occurring in 1956 and 3 major trials occurring in 1957. These major tests each featured different designs, though both sites; One Tree (OT) and Breakaway (B), had "Red Beards" tested at their location. The "Red Beards" are a type of nuclear bomb design that featured a ^{235}U and ^{239}Pu enriched core, which resulted in a large explosive yield recorded at 15kt of TNT for OT and 10kt of TNT for B (MRTAC, 2003). This caused any contamination from the subsequent explosion to be dispersed over a significantly large area unlike the minor tests, which had contamination focused around a small area near the detonation. Site Tadje (T) was the location of a different type of bomb called a "Pixie", which had a smaller explosive yield of 1kt of TNT. This design featured a solely ^{239}Pu core (Archive, 2007). Figure 1 presents a layout of the mentioned sites within SA and their locations within the region.

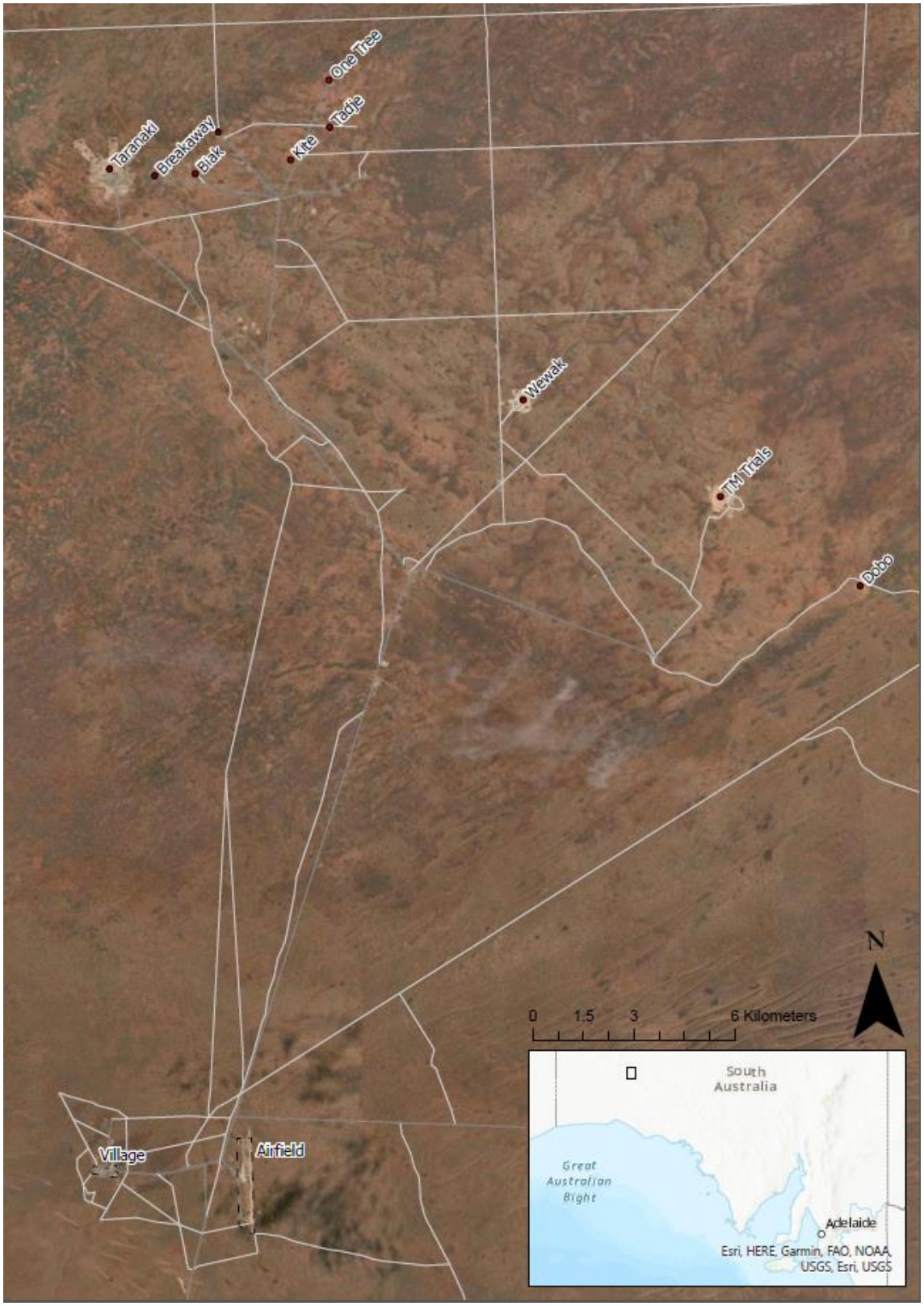

Figure 1: The site layout of the Maralinga nuclear operation with approximate locations of the various test sites and areas of operation.

Techniques to map and constrain areas that have been exposed to nuclear contamination using radioactive isotopes, also known as radionuclides, has developed significantly over the last few decades due to advancing concerns regarding prolonged radioactive contamination in the environment and due to the development of new analytical instrumentation. Historical nuclear testing locations serve as a great example of potentially widespread contamination and provide ideal conditions to test and develop new analytical techniques. Detonation of many nuclear prototypes and numerous minor tests caused soil contamination across multiple sites within Maralinga; and most sites contain contamination that can still be detected today through the presence of long-lived radionuclides such as plutonium (^{239}Pu) and americium (^{241}Am), (Lokan, 1985). In addition, the radioactive caesium (^{137}Cs) is the most well-known moderately lived fission product, formed from decay of ^{235}U, which can still be detected across many sites (Boulyga & Becker, 2002). Europium (^{152}Eu) also serves as another moderately lived radionuclide which can be used to trace fission of ^{235}U (Boulyga & Becker, 2002). Other short-lived radionuclides such as cobalt (^{60}Co), which was used in minor trials, is no longer present at a significant level to warrant environmental or health concerns (SRP, 2022). All mentioned radionuclides and their half lives are given in Table 1.

MAN-MADE ISOTOPE	Half-life (years)
^{60}Co	5.271
^{137}Cs	30.19
^{152}Eu	13.5
^{239}Pu	24,065
^{241}Am	432.2

Table 1: A list of mentioned radionuclides along with their name and half-life (Loebe, 2014; UAB, 2003)

The lack of communication and knowledge at the time of the trials was key to causing this level of widespread radionuclide contamination, which was further exasperated by poor clean-up attempts by the British (MRTAC, 2003). The predominant risk present at Maralinga to humans currently, is through the inhalation and ingestion of 'hot' particles (Cook et al., 2021). These micron-sized particles were widely distributed during detonation and consist of long-lived radionuclides, predominantly plutonium and uranium. Particles matching this common description have been identified at Maralinga in literature (Cook et al., 2021; Cooper et al., 1994; Ikeda-Ohno et al., 2016).

Many nuclear applications and military tests required fissile isotopes; these fissile isotopes undergo fission through the capture of neutrons. Most commonly these applications were focused on the ^{235}U isotope. One of ^{235}U's multiple fission pathways is responsible for generating ^{137}Cs, which is shown in Figure 2. Natural uranium is required to undergo an enrichment process as its predominant isotope ^{238}U, makes up >99.27% of natural uranium (Alloway, 2013). Enriched uranium is the major component in the nuclear prototypes used in the major tests, with estimated enrichments for weapon grade U being >90% of ^{235}U. Comparatively, nuclear fuel, used in reactors, only contains ~2% of ^{235}U enrichment (Nuclear, 2022). The nuclear contamination (man-made) should thus be identifiable by a higher abundance of ^{235}U relative to the main ^{238}U isotope. Increased enrichment levels in contaminated soil would not only provide insight into the extent of the affected area but would provide insight into the enrichment grade of ^{235}U used in the tests performed at Maralinga.

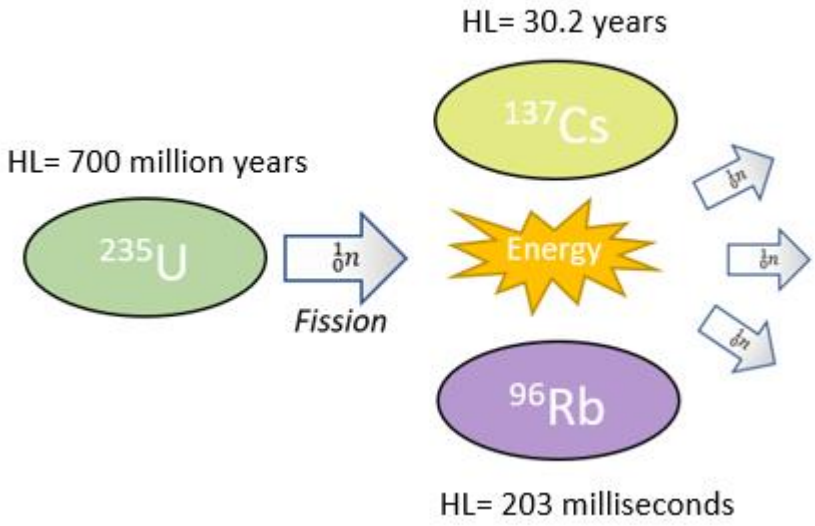

Figure 2: One pathway ^{235}U can undergo during fission to generate relatively short-lived ^{137}Cs and ^{96}Rb radionuclides as products and continue the cascade of neutron generation, which can then aid other fissile elements in their fissile pathways, paired with the half-lives (HL) of each isotope.

Numerous different radionuclides are found within radionuclide contaminated areas due to the large number of possible fission and decay pathways. The large variety of radionuclides present provides many possible radionuclides, which can serve as tracers for the contamination. As previously mentioned ^{137}Cs remains incredibly useful for ^{235}U fission tracing (Lal et al., 2017). The use of ^{239}Pu as a fissile element in these nuclear tests can be tracked through the presence of ^{241}Am (Boulyga & Becker, 2002) . Figure 3 demonstrates the decay pathways of ^{239}Pu used in these tests and the generation of ^{241}Am. Highly enriched ^{239}Pu was cheaper to produce than highly enriched ^{235}U thus, detection of ^{239}Pu and its various products is crucial due to its abundant usage (Johnston, 1988). ^{239}Pu undergoes alpha decay, which has a short detection distance and can be inferred due to the presence of ^{241}Am (Ikeda-Ohno et al., 2016). ^{241}Am can be detected over larger distances due to its gamma ray decay line. Additionally, this

radionuclide has a half-life of 432.2 years, allowing it to act as a tracer for significant periods of time (Johnston, 1988).

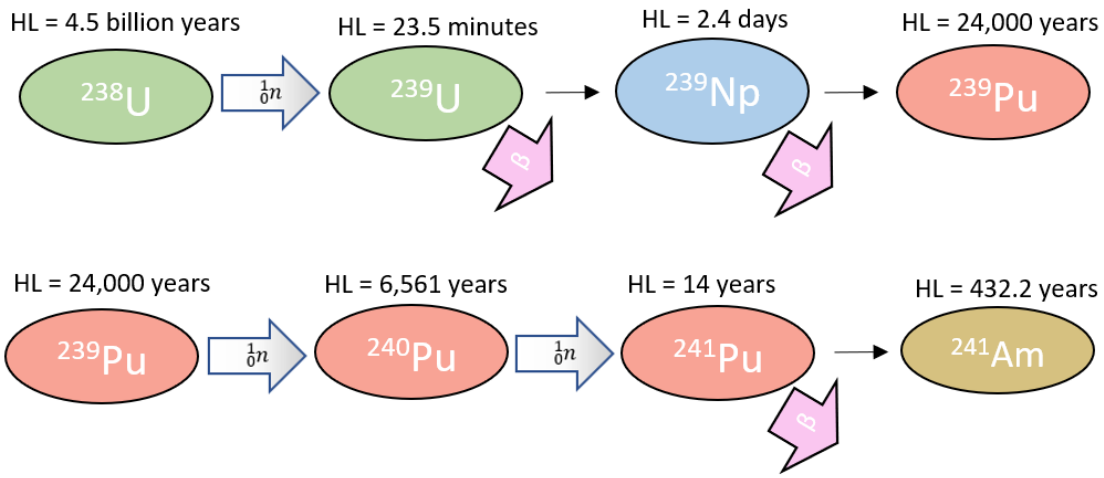

Figure 3: The pathway of artificially generating ^{239}Pu from ^{238}U and how ^{241}Am is generated from ^{239}Pu. The first line demonstrates the method of generating the artificial ^{239}Pu from ^{238}U used in the tests. The second line however shows the generated ^{239}Pu gaining neutrons during fission to become ^{241}Pu, which then decays to ^{241}Am. Each isotope is paired with its respective half-life (HL).

This research seeks to use the ^{235}U/^{238}U isotopic ratio obtained from Maralinga soil as well as control samples from various natural sources, to generate data that can provide constraints to the area of man-made nuclear contamination across the Maralinga sites. Distribution of contamination is predominantly wind dependent and thus is subject to be distributed further over time (MRTAC, 2003). Figure 4 demonstrates the aims of the experiment as identification of ^{235}U enriched 'Hot' particles is crucial to confirming the presence of contamination within the Maralinga samples. Induction coupled plasma mass spectrometry (ICP-MS/MS) then can be used for detection of uranium isotopes within samples with gamma spectroscopy (GS) providing information on the various radionuclide contamination. Solution ICP-MS/MS can be used to precisely measure atomic concentrations of a bulk soil sample. As GS measures the total radionuclide contents of a sample ICP-MS/MS provides a greater specificity of uranium isotope data for bulk soils

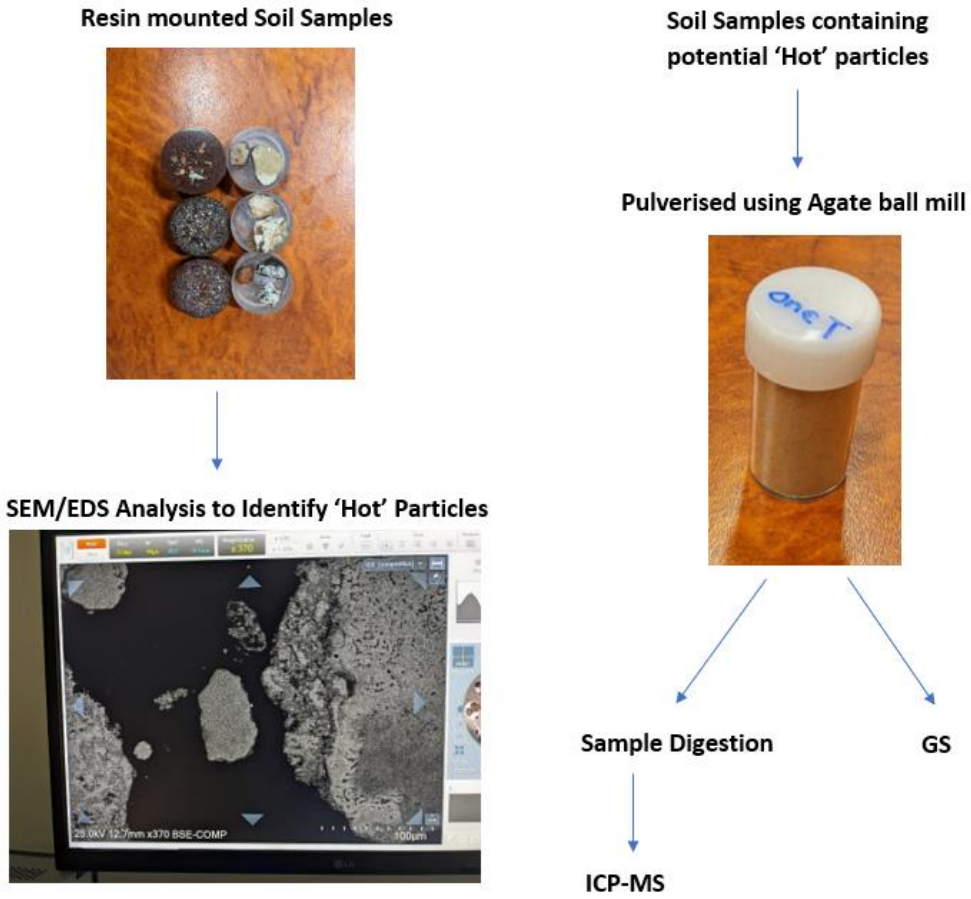

Figure 4: A schematic diagram illustrating the procedure used for identification and analysis of samples.

2. BACKGROUND

2.1 Contamination by man-made radionuclides at Maralinga

The decrease in contamination of long-lived radionuclides present today is a result of the numerous clean-up attempts performed at Maralinga, and partly also due to the natural decay of these radioisotopes over the past decades. Many other radionuclides such as ^{210}Po, ^{60}Co, and ^{46}Sc were also scattered throughout the region during minor trials but due to their short half-lives they no longer pose an issue or health concerns and have become undetectable over the 60 years since the trials ended (Goldstein et al., 2021). The long-lived radionuclides and moderately lived radionuclides are still present

at low levels within the topsoil and would be found in disequilibria with their daughter products as many have yet to reach their half-lives since their artificial introduction into the environment. This disequilibrium impacts the ability to infer concentrations of long-lived radionuclides through their daughter products. Fortunately, the mobility of primary contamination is limited due to the weather conditions and soil present at Maralinga (James, 1988). The major form of transport for contamination is through wind, which also poses the risk of inhalation of 'hot' particles from the created dust. Due to the low rainfall and the low solubility of plutonium, its downward mobility is very limited, with a penetration rate of 2-3mm per year (Johansen et al., 2014). Unlike plutonium, uranium is more mobile and toxic when oxidised allowing it to remain in porewater (Oliver et al., 2008)

To investigate the scale of contamination the Technical Assessment Group (TAG), a group set up by the Australian government and tasked with remediation of the area, completed an aerial radiological survey in 1987 (MRTAC, 2003). The data they collected confirmed the presence of ^{241}Am, ^{137}Cs, ^{60}Co and ^{152}Eu near 'ground zero' or the sites of detonations, with radionuclide contamination carried along wind carried plume paths from the sites. ^{235}U and ^{238}U isotopes were both undetected in these areas by earlier studies (MRTAC, 2003). The 12 Vixen B trials are the cause of the greatest contamination across any of Maralinga's site. They occurred at site Taranaki (TA) and dispersed 22kg of plutonium and a similar amount of ^{235}U, which was then carried by wind (MRTAC, 2003). As a result, three long plumes to the north-east, north-west, and north were created and characterised by their ^{241}Am activity, and these are illustrated in Figure 5.

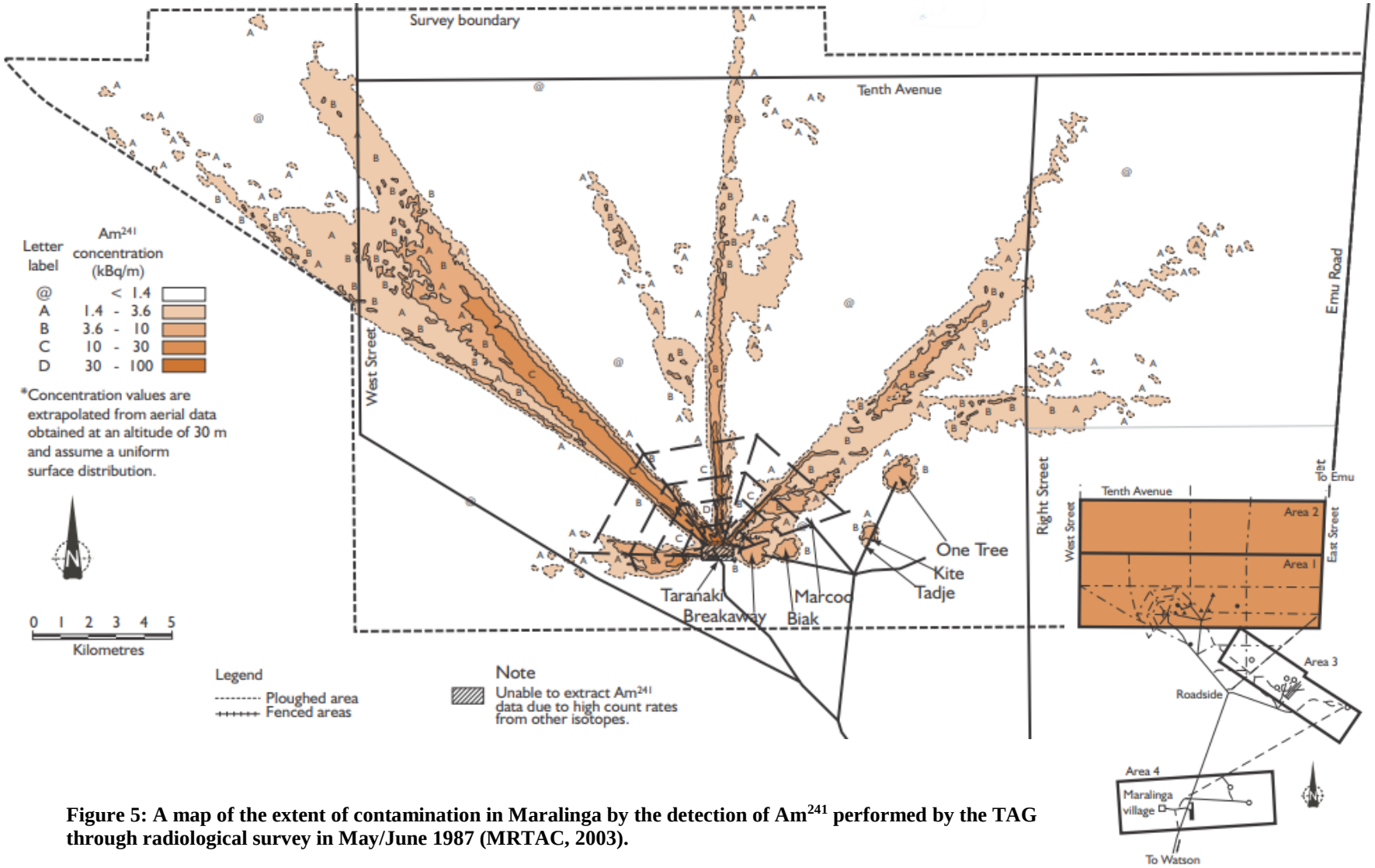

Figure 5: A map of the extent of contamination in Maralinga by the detection of Am^{241} performed by the TAG through radiological survey in May/June 1987 (MRTAC, 2003).

The British organised and orchestrated three clean up attempts at the Maralinga sites, with the most significant occurring in 1967. This major program was titled Operation Brumby and it focused on cleaning up the severely contaminated soils at the minor test sites and the major test site, TA, which is found adjacent to site B. It involved ploughing contaminated soil to a depth of 10 cm to dilute the radioactive material in the surface soil (Lokan, 1985). *In-situ* vitrification (ISV), a method of melting and cooling buried material into a 'glassy rock' mass to limit mobility of contamination, was suggested at the time by the TAG as another method for suitable clean-up for extremely contaminated material. Damage, during use, to the ISV machinery resulted in only 11 of the 21 pits at TA to be treated (MRTAC, 2003). The process also had numerous shortcomings with vaporisation of material causing loss and inhalation at the time and downward migration of material through cracks, which formed through improper cooling of the vitrified rock (MRTAC, 2003). These two major efforts were unsuccessful resulting in greater clean-up efforts being required later.

A total of 150ha , 29 ha, and 46 ha of topsoil was removed from sites TA, Wewak and TM100/TM10 respectively and buried in designated trenches with a cap of 5 m of uncontaminated rock; additional pits were also created at the airfield and cemetery from transported material (Lokan, 1985). MRTAC enforced a clean-up criterion that varied for each site with a specific activity limit on the average ^{241}Am level found in the topsoil per hectare. Major criteria across all sites stated that all particles and fragments of contamination did not exceed 100kBq ^{241}Am, and that particles of activity greater than 20kBq ^{241}Am would not exceed a density of 0.1 per m^2 throughout the topsoil. (MRTAC, 2003).

2.2 Natural Uranium isotopes

Uranium has 3 naturally occurring radioactive isotopes in the form of ^{234}U, ^{235}U, and ^{238}U. In addition, ^{233}U and ^{236}U are man-made isotopes found in reprocessed nuclear material. Ideally this can serve as a tracer for nuclear uranium contamination, if detectable. ^{235}U is the only fissile isotope of these 4 and thus, an enrichment of ^{235}U is needed to undergo nuclear fission. Enrichment for nuclear grade uranium requires it to be >90% of ^{235}U and for nuclear reactor fuel is commonly enriched with ~3-5% of ^{235}U (Nuclear, 2022). Thus, based on the abundance of ^{235}U relative to the main ^{238}U isotope in the sample of interest the source and purpose of the uranium can be inferred. The $^{235}U/^{238}U$ isotopic ratio of natural uranium is ~0.00725. CRM 145 serves as a recognised standard of natural uranium isotopic composition and thus contains this $^{235}U/^{238}U$ isotopic ratio listed in Table 2. Further standards used include CRM-U010, CRM U500 and CRM U0002.

By using two standards when performing a solution ICP-MS/MS analysis, one can constrain the $^{235}U/^{238}U$ isotopic ratio to an unknown sample; and a double spiking method can also be applied to further improve the data quality and precision (Mathew et al., 2013). All standards mentioned and used in testing are displayed in Table 2.

Standard	^{234}U	^{235}U	^{236}U	^{238}U	$^{235}U/^{238}U$	*Source*
CRM U0002	0.00016	0.01755	<0.00001	99.9823	0.00018	The Adelaide University
CRM 145	0.0052458	0.72017	-	99.27458	0.00725	Macquarie University
CRM U010	0.00541	1.0037	0.00681	98.984	0.01014	Macquarie University
CRM U500	0.5181	49.696	0.0755	49.711	0.99970	Macquarie University

Table 2: The uranium standards used throughout this study and their certified uranium isotope abundances in atom percent as well as the institutes from where they have been sourced from for this study. (Neuhoff, 1987, 2008a, 2008b, 2010)

2.3 Previous uranium isotope characterisation and mobility

Usage of isotope ratios to constrain the mobility of uranium for weapons testing sites have previously been investigated at the MoD weapons testing range (Oliver et al., 2008). Samples of earthworms, porewater and soil were collected to monitor the mobility of depleted uranium sources. Uranium mobility varies greatly depending on the environment of the soil with various ligands and pH, that can hinder or assist in the mobility of uranium (Cumberland et al., 2016). The Depleted uranium sources were in greater abundance, at greater distances, within porewater and earthworm tissue (Oliver et al., 2008). The transport of uranium within water and fauna is minimal at Maralinga due to its arid conditions. Furthermore, diffraction of uranium isotopes in the environment is negligible due to each isotope having a relatively small mass difference between each other (Hill et al., 2020). ‘Hot’ particles have been shown to contain uranium and thus may provide a similar constraint on uranium isotope ratios when measured (Cook et al., 2021).

2.4 Additional radionuclides and man-made isotopes

Plutonium is an artificial element with its isotope, ^{239}Pu, being used in nuclear weapons due to being a fissile isotope like ^{235}U. As shown in Figure 3, ^{239}Pu through neutron capture becomes ^{241}Pu, which then decays to ^{241}Am. As previously mentioned, ^{241}Am is present at nuclear contaminated areas and is more easily detected than ^{239}Pu due to its shorter half-life and thus detectable gamma decay pathway. Plutonium, though harder to detect, still serves as a long lived tracer for nuclear contamination, with ^{239}Pu having a half-life of 24,110 years, (Browne, 2003; Browne & Tuli, 2007). While ^{241}Am is beneficial for inferring material sourced from ^{239}Pu it is possible that not all sites had ^{239}Pu that underwent fission and thus, would have an absence of ^{241}Am (Lal et al., 2017). This is not important for major trials, where samples have been collected from, as experiments performed there were built to undergo fission (Parkinson, 2004).

^{137}Cs has been heavily used as a tracer in soils affected by nuclear testing and contamination, as it is created from fission of ^{235}U. ^{137}Cs has a high affinity for adsorbing to soil particles and has a low solubility in water causing it to remain attached to soils for long periods of time (Tims et al., 2016), and also because it follows geochemical pathways of potassium (K), the latter being a prominent nutrient element for plants and vegetation. ^{137}Cs however, has a physical half-life of 30.08 years meaning that only a quarter of original ^{137}Cs is present at Maralinga today (Browne & Tuli, 2007). The hundreds of minor tests that were the significant cause of contamination of additional radiogenic species have been split into the 6 categories, which are listed below in Table 3, with the amounts of the major radionuclides used listed.

Minor Trial	*Location*	*^{239}Pu (kg)*	*^{238}U (kg)*	*^{210}Po (TBq)*	*^{46}Sc (TBq)*	*^{212}Pb (TBq)*	*Be (kg)*
Kittens	Naya 2	-	120 CORN	210 CORN	-	-	0.75 CORN
Tims	TM100/101	1.2 SCHO	172 CORN	-	-	-	-
	Kuli	-	7400 SCHO	-	-	-	>28 SCHO
		-	7700 CORN	-	-	-	70 CORN
	TM50	-	90 SCHO	-	-	-	9 SCHO, 10 CART
		-	-	-	-	-	
Rats	Dobo	-	26 SCHO	-	3.7 CORN	4.4 CORN	-
		-	28 CORN	-	-	-	-
	Naya	-	150 SCHO	15 SCHO	75 CORN	-	-
		-	170 CORN	-	-	-	-
Vixen A – fire	Wewak	0.41 SCHO	40 CORN, 4.8 STEW	-	-	-	4.5 STEW
Vixen A – explosion		0.57 SCHO	>17 CORN	-	-	-	3.5 STEW
Vixen B	TA	22 SCHO	22 CORN	-	-	-	18 CORN
		-	24 #CORN	-	-	-	-

Table 3: Rounded estimates of radioactive and toxic materials used in the minor trials. With the official name of the trial paired with the location and the weight of the various nuclides that were included in the tests. (#) experiment also included enriched uranium. A – (Schofield 1985). B – (Carter 1985). C - (Cornish 1986). D - (Stewart 1960).

3. METHODS AND SAMPLES

3.1 Sample Collection

Three Maralinga soil samples were provided for this study by the SA EPA with limited information on the site location information and coordinates from where they were collected. The samples (~300g each) were broadly localised from the sites T, B, and OT; all of which were the location of a major trial. These 3 Maralinga samples contained a mix of rock chips, rootlets, and very fine-grained dust. Additionally, a 100g soil sample from rural Coober Pedy (CP) sourced by Jarrah Mik (CRREI, University of Adelaide) and 50g of a high purity uraninite (UITE) obtained from the Mawson Tate Museum, originally from Bohemia (Czech Republic), were also obtained and investigated in this study as local 'reference materials' for the natural U isotopic ratio or the background composition. The CP sample provided had already been pulverised to a very fine-grained powder. All soil samples were handled using gloves and a P2 mask and processed at the Mawson sample preparation and Bruce Geochemistry Clean laboratories

3.2 Sample Preparation

A mix of powder and rock chips totalling to 100g of each (i.e., representing an individual Maralinga sample) was pulverised using a FRITSCH 'pulverisette 0' agate ball mill. Samples were loaded in ~25g portions and ran for ~30-45min until they reached a homogenous very fine-grained powder. This was also done for UITE, which consisted entirely of rock chips. A total of 200µg of pulverised CP, B, OT, and T underwent acid digestion in accordance with the method described in Appendix C, and afterwards they were evaporation and redissolved using 2% HNO_3 with a dilution factor

of 1/50. Due to the high concentration of uranium in UITE, only 10µg of pulverised sample was used in its digestion and diluted to a factor of 1/500. All sample weights and dilutions were recorded using a Mettler Toledo six-digit balance at Mawson Laboratories.

3.3 SEM-EDS Imaging and Mineral Mapping

One inch resin mounts of both rock chips and soils were prepared from T, OT, and B samples. The six mounts were carbon coated and analysed under the SU3800 Hitachi scanning electron microscope (SEM). The SEM uses energy dispersive spectrometry (EDS) to identify minerals, providing micro-scale mineral maps of analysed samples/ mounts. Increasing the contrast of the scan allows heavier elements to become more visible, as lighter, or bright white areas. A large grain of galena present in the B soil sample was used as a contrast threshold with all grains that exceed this level to be identifying and scanned using SEM-EDS.

3.4 Solution ICP-MS/MS

Three ICP-MS/MS (Agilent 8900) experiments were performed at Adelaide Microscopy (University of Adelaide, SA). These experiments focused on determining and measuring the ^{235}U /^{238}U isotope ratios of the various samples and standards. The measured isotopic ratios ($^{235}U/^{238}U$) were normalised using certified reference materials and the calculated and corrected isotope ratios (see also Equation 1, below) are presented in the following sections. The initial ICP-MS/MS experiment was performed using a 1/1000 dilution factor for all soil samples and both a 1/5,000 and 1/5,000,000 dilution factor for UITE. The isotope abundances of ^{235}U and ^{238}U were measured as isotopic ratios using an internal ICP Mixed-A-standard. The initial experiment

identified that a dilution of 1/5,000,000 for UITE and that a lower dilution factor of 1/750 for all other samples would place the uranium concentration in the ideal range for the higher precision 'pulse' mode of the ICP-MS/MS instrument. The 2nd experiment was performed using the certified isotope standards CRM145, CRM U010, CRM U0002, and CRM U500 with each diluted to uranium concentrations of 100ppb and 10ppb for 'analog' mode and 'pulse' mode respectively. Having standards in range of both 'analog' and 'pulse' mode allowed a conversion factor to be calculated between modes to further strengthen the robustness of the data and results, but still provide an accurate reading if the sample was tested using the less precise 'analog' mode. Furthermore, the unknown samples have been bracketed by known and certified uranium isotope standards in the analytical sequence, using a commonly applied 'sample-standard bracketing' (SSB) technique. This approach allows the known standards to be used as references for unknown samples and to calculate

$$\frac{Standard's\ Experimental\ \frac{^{235}\mathrm{U}}{^{238}\mathrm{U}}\ ratio}{Standard's\ Known\ \frac{^{235}\mathrm{U}}{^{238}\mathrm{U}}\ ratio} \times \frac{^{235}\mathrm{U}}{^{238}\mathrm{U}}\ ratio\ of\ sample = Corrected\ \frac{^{235}\mathrm{U}}{^{238}\mathrm{U}}\ ratio\ of\ sample$$

the above-mentioned correction factor, and thus corrected U isotope ratios, using the equations shown below:

Equation 1: Formula used for the calculation of corrected uranium isotope ratios based on a known uranium isotopic standard.

The second experiment using the above listed U isotope standards was to test the margins of error or uncertainty associated with the isotope ratios ($^{235}U/^{238}U$) and the U concentration measurements, using certified data and results obtained from Macquarie University. Standards with the smallest margins of error from their known U isotopic ratios were chosen as reference standards to have unknown samples bracketed against them in the 3rd experiment or ICP-MS/MS analytical session. This 3rd experiment was performed with only CRM U500 and CRM U010 isotope reference standards at a concentration of 10ppb of U.

Note that CRM 145 and CRM U0002 were not included in this third trial due to issues with their reproducibility.

3.5 GS analysis of radionuclides

Samples of powdered material from B, OT, T, CP, and UITE were manually compressed using a Teflon rod into 2 cm diameter plastic tubes up to a height of 4cm, and the tubes sealed with hot glue. Sealing and compression of each sample was done to reduce the amount of empty space between the grains and to remove air pockets which allow for the build-up of radon gas from the uranium decay chain. This removes interference with the homogeneity of the gamma rays emitted from the sample, while the hot glue seal prevents any external gas loss.

Samples were left sealed for one week before being tested, to generate and equilibrate the build-up of radon gas with its decay chain within the samples. The use of the specific thin long plastic tube allows the emitted gamma rays to travel through only a small amount of sample before reaching the detector without losing significant energy. Detection was performed using a liquid nitrogen cooled, high purity germanium radiation detector from ORTEC. Background radiation was minimised using a high performance ultra-low background lead shield (HPULBLS) from ORTEC. Measurements were recorded over 3 days and produced an absorption spectrum of all measured gamma rays. Various radionuclides and isotopes of interest were detected and then identified from their corresponding gamma ray energy in the absorption spectrum using Genie 2000 software (with assistance from Dr Chris Kalnins and Dr Joseph Builth-Williams) at Centre for Radiation Research Education and Innovation CRREI, University of Adelaide.

4. RESULTS

4.1 HOT PARTICLE IDENTIFICATION

SEM-EDS imaging provided the identification of numerous small particles and mineralogies present within the soil samples T, OT, and B, all of which consisted of uranium oxide and thus, identified as ‘Hot’ particles (Cook et al., 2021). The full SEM-EDS scans were only completed with the soil mounts as the test sections performed on the rock chip mounts did not contain any detectable ‘Hot’ particles with high contrast. The X-ray spectra collected from 2 seperate ‘Hot’ particles during the SEM-EDS session are present in Appendix D. These particles ranged in size from 1-10µm with smaller particles not being identified during the bright phase screening due to the resolution limit. These particles match the size limit range described in previous literature; however, they possess no identifiable plutonium enrichment (Cook et al., 2021; Cooper et al., 1994; Ikeda-Ohno et al., 2016).

The ‘Hot’ particles did not possess any irregularities in composition and appeared rather homogenous with the resolution used. Particles appear both loose within the soil matrix, such as in Figure 6 (A), and also adhered to grains as visible in Figure 6 (B). The particles were extremely sparsely populated throughout each sample with sample B containing the greatest abundance. There was a greater abundance of grains loose throughout the mounts rather than grains that were adhered to larger grains. All Maralinga samples consisted of fine-grained and carbonate rich soils and no noticeable trend that could be observed between adsorption of ‘Hot’ particles to the dominant carbonate grains compared to less abundant quartz grains.

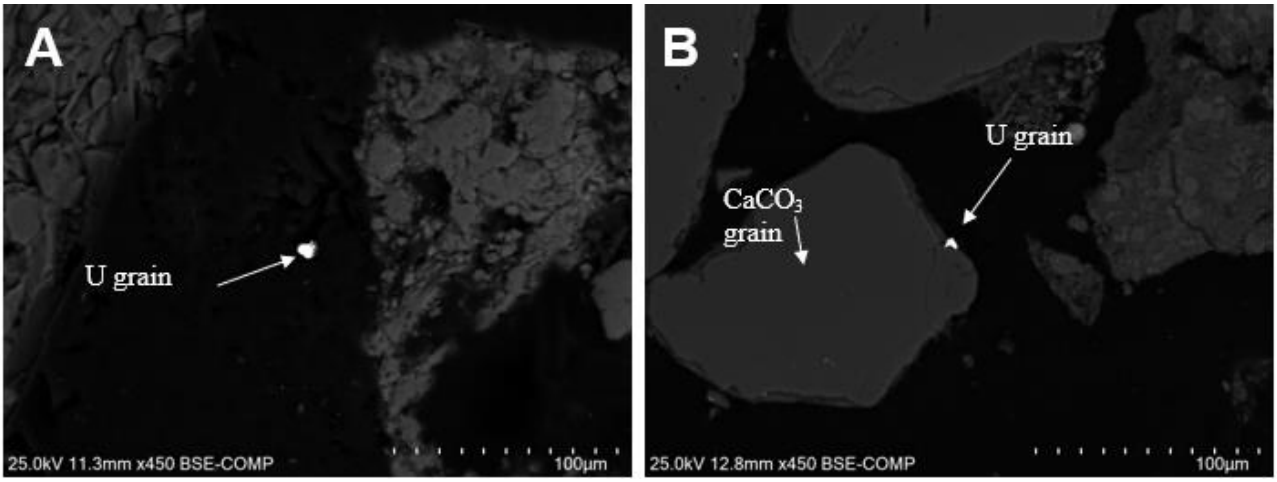

Figure 6: (A) A SEM image of a resin mounted soil sample from site T with a uranium-rich grain freely distributed within the sample matrix. (B) A SEM image of a resin mounted soil sample from site B with a uranium-rich grain present as adhered 'Hot' particle attached to a calcium carbonate grain/clast.

4.2 URANIUM CONCENTRATION

Solution ICP-MS/MS data confirmed extremely low concentrations of U across all samples analysed from the Maralinga site. Sample UITE, contained expected high abundances of uranium with an average of 212,996 ± 551 ppm giving it a ore grade of slightly more than 20% uranium oxide, expected of uraninite. Sample B was the only sample from Maralinga with a concentration of uranium greater than 1ppm, at 10.0 ± 0.3 ppm. This coincides with B also containing the greatest number of uranium-rich 'Hot' particles of all the Maralinga samples analysed and screened with the SEM-EDS. For the above measurements, the 'Mixed A standard' was used for construction of calibration curve for U concentrations, and details can be found in Appendix A.

Isotopes ^{234}U, ^{236}U, and ^{241}Am were also analysed for isotope abundances using ICP-MS/MS from the samples B, OT, and T. The measured isotopes abundances of the above-mentioned radionuclides all fell below detection limit and thus, were excluded from further analysis and discussion in the ICP-MS/MS experiments. Finally, ^{239}Pu was

also tested as a possible target for investigation using the ICP-MS/MS approach but due to interference issues ($^{238}U + {}^{1}H$ = interference on mass 239) and a lack of a suitable ^{239}Pu concentration or isotope standard in this study, the analysis of ^{239}Pu was excluded from the testing. Hence, without a method to directly obtain ^{239}Pu measurements via mass spectrometry, ^{241}Am measurements obtained from GS served to identify and indirectly infer the presence of ^{239}Pu in the samples.

4.3 URANIUM ISOTOPE RATIOS VIA ICP-MS/MS

The measured and corrected (i.e., normalised) ^{235}U /^{238}U isotope ratios (ppm/ppm) for all studied samples are shown in Figure 7. The natural uranium isotope ratio (based on CRM 145's official isotopic value) is also plotted as the example of natural background values. Two certified uranium isotope standards used for data normalisation include CRM U010 and CRM U500, which are significantly more enrichmed in ^{235}U and thus, cannot be effectively plotted or shown in Figure 7 (as their values are off the scale). All Maralinga soil samples, as well as CP and UITE resulted in having a quasi-natural $^{235}U/^{238}U$ isotopic ratios, in agreement with the natural uranium isotope composition, characterised by CRM 145. All samples besides B2 plotted within such natural $^{235}U/^{238}U$ isotope ratio of 0.00725, within their 95% confidence intervals. The measured samples had an average error of 0.14%. All duplicate samples for CP, B, OT and T contained the sample stock solution (i.e., parent dilution material) and thus, any variation observed between duplicates was due to measurement uncertainty and analytical conditions related to the detectors, instrument stability, etc.

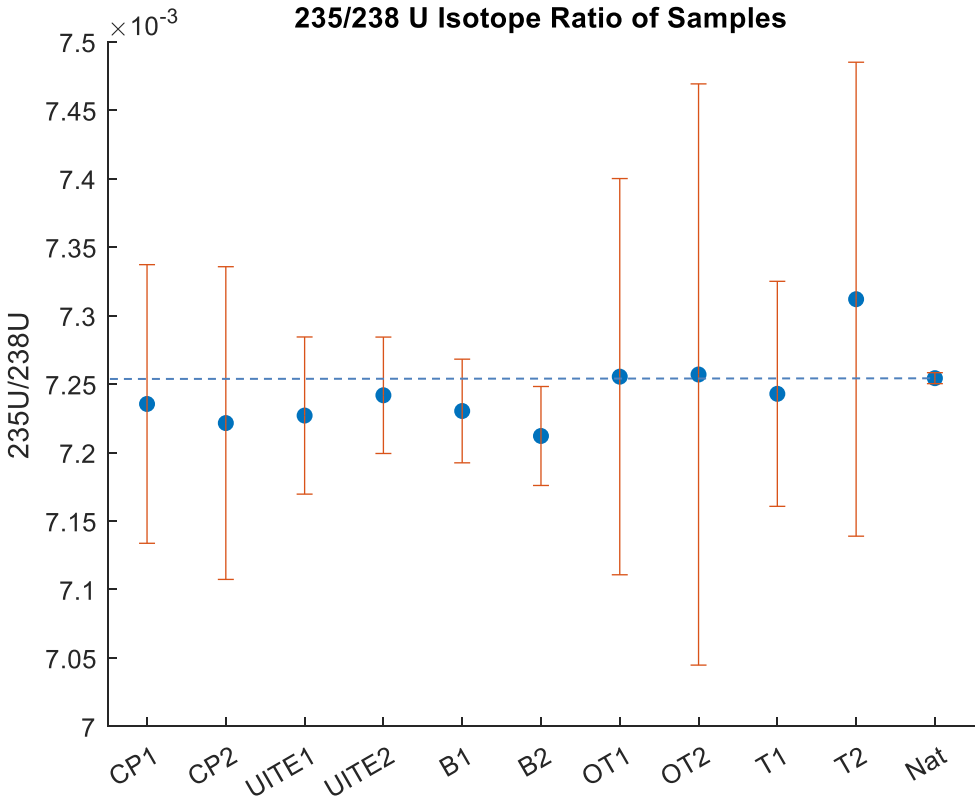

Figure 7: he $^{235}U/^{238}U$ isotope data (corrected ratios) acquired from analysed samples and their respective uncertainties (error bars) as determined for samples duplicate runs. The horizonal dashed line illustrates 'natural' U isotope reference line, based on the known ^{235}U /^{238}U isotope ratio in CRM 145 standard.

4.3 GS OF MAN-MADE RADIONUCLIDE/ISOTOPES

The weight mean activity and the minimum detectable activity (MDA) of each sample was determined with a 95% confidence interval from GS analysis (Thangam et al., 2022). The weight mean activity was used for ^{235}U isotopes and other radionuclide level determination as it was most representative of the bulk soil and could be more readily contrasted against the data acquired from ICP-MS/MS analysis of identical samples. The Maralinga soil samples each contain one or more of the man-made radionuclides ^{137}Cs, ^{152}Eu, and ^{241}Am. As expected, both naturally sourced uranium samples (CP and UITE) have an absence of these man-made isotopes as illustrated in Figure 8A-E. The Maralinga soil samples contained no significant excess of ^{235}U when compared to

natural or reference sample CP. No ^{235}U was detected in sample B, likely due to an error in detection or misreading of the gamma absorption spectra. The natural gamma radiation emitted by ^{235}U in sample CP is at a similar level to samples OT and T as shown in Figure 8F. The confidence interval of sample CP for ^{235}U isotope abundance has a greater level of precision when compared to samples OT and T, which is due to the lower background radiation present in the uncontaminated sample. Interpretation of the absorption spectra was not fully completed as some energy peaks corresponding to less common radionuclides were not identified. A variety of other radionuclides besides those 4 listed below were detected, and these are listed in Appendix D.

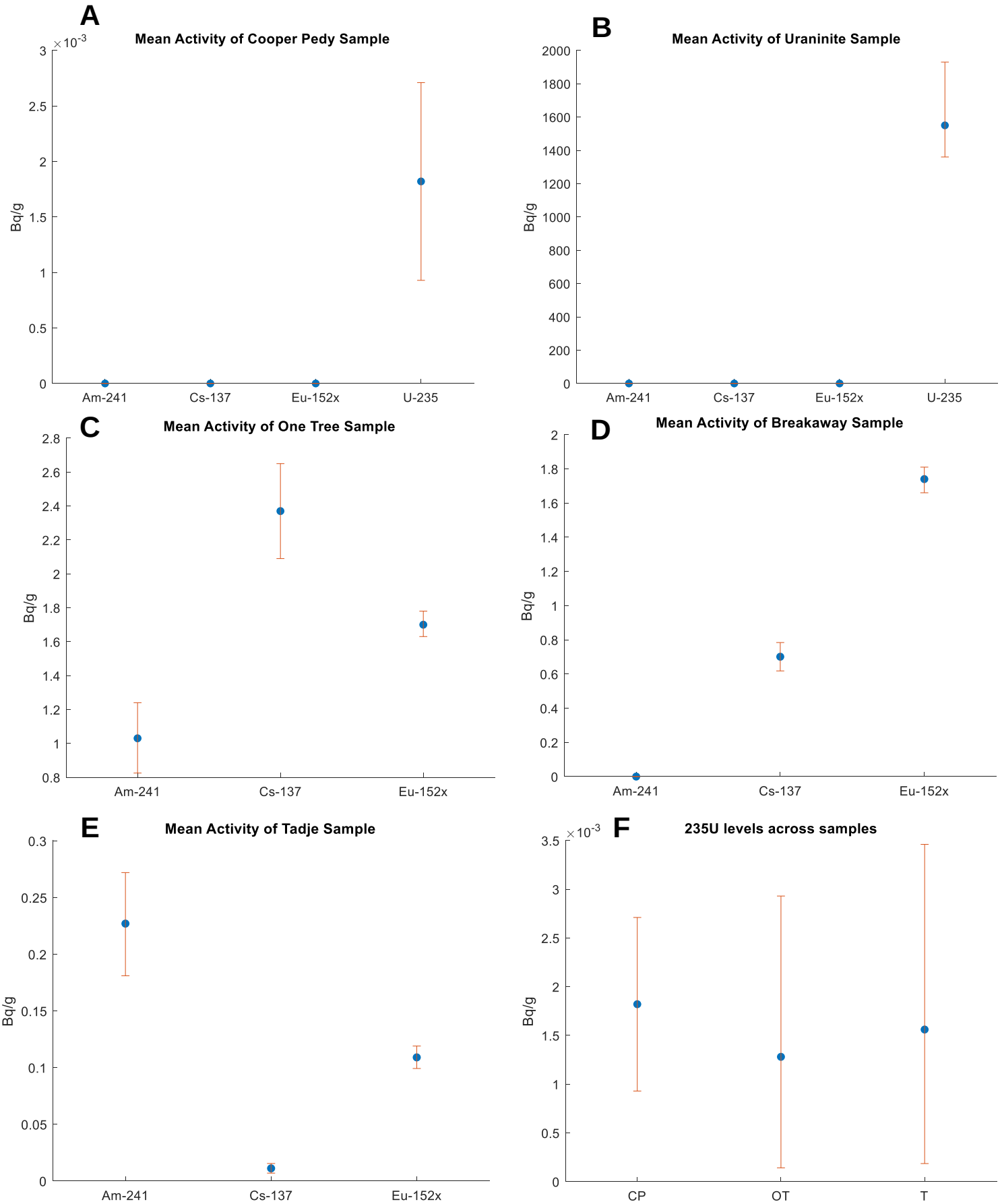

Figure 8: A-B: The measured presence of activity in Bq/g of the elements ^{235}U, ^{137}Cs, ^{152}Eu, and ^{241}Am for the uncontaminated samples CP and UITE using GS.

C-E: The measured presence of activity in Bq/g of the elements ^{137}Cs, ^{152}Eu, and ^{241}Am for the contaminated Maralinga samples using GS.

F: A comparison of the ^{235}U level of the natural CP against the levels obtained for the contaminated OT and T.

5. DISCUSSION

5.1 Comparing data from GS and ICP-MS/MS

The usage of ICP-MS to directly measure all uranium isotopes had a wide range of variability between samples, which was dependent on the abundance of uranium found within each sample. As shown by samples OT & T provided larger error bars than sample B. Indirect measurement of ^{235}U through its activity using GS provided an additional method to confirm the presence of ^{235}U enrichment however, both techniques did not provide any clearly visible enrichment in ^{235}U, as shown in Figures 7 and 8F. These two techniques are not directly comparable but using calculations, conversions can be made between the two techniques for uranium concentrations and activity of uranium. Using the known activity values emitted by the various uranium isotopes, the ^{238}U Bq/g sourced radiation (in Bq/g) can be calculated using the measured ^{235}U activity obtained from GS, while assuming that the ^{235}U /^{238}U ratio of the sample is natural or close to natural composition (as confirmed by ICP-MS/MS. As all investigated samples yielded such a quasi-natural uranium isotopic ratio, the conversion remains the same for all samples.

$$^{235}\mathrm{U(Bq/g)} \times 2.175 = {}^{238}\mathrm{U(Bq/g)}$$

Equation 2: Conversion of ^{235}U to ^{238}U (in Bq/g) from GS readings (Equation supplied by Dr Chris Kalnins).

Further calculations can be performed using the calculated Bq/g values of samples to determine the corresponding uranium concentration (in ppm) from Bq/g, and vice versa, thus allowing a direct comparison of the two methods used (GS and ICP-MS/MS), (WISE Uranium, 2018). Data shown in Table 4 was used to calculate the concentration of uranium (in ppm) for the GS data (in Bq/g), as shown in Figure 9.

Sample	*Total U concentration from ICP-MS (ppm)*	*^{235}U GS reading (Bq/g)*
OT	0.3665567	0.01
T	0.3761063	0.0034
B	10.04666	-
CP	0.5572562	0.0040
UITE	212996.09	3371.25

Table 4: uranium concentration data and Gamma ray data obtained from ICP-MS/MS and GS, respectively.

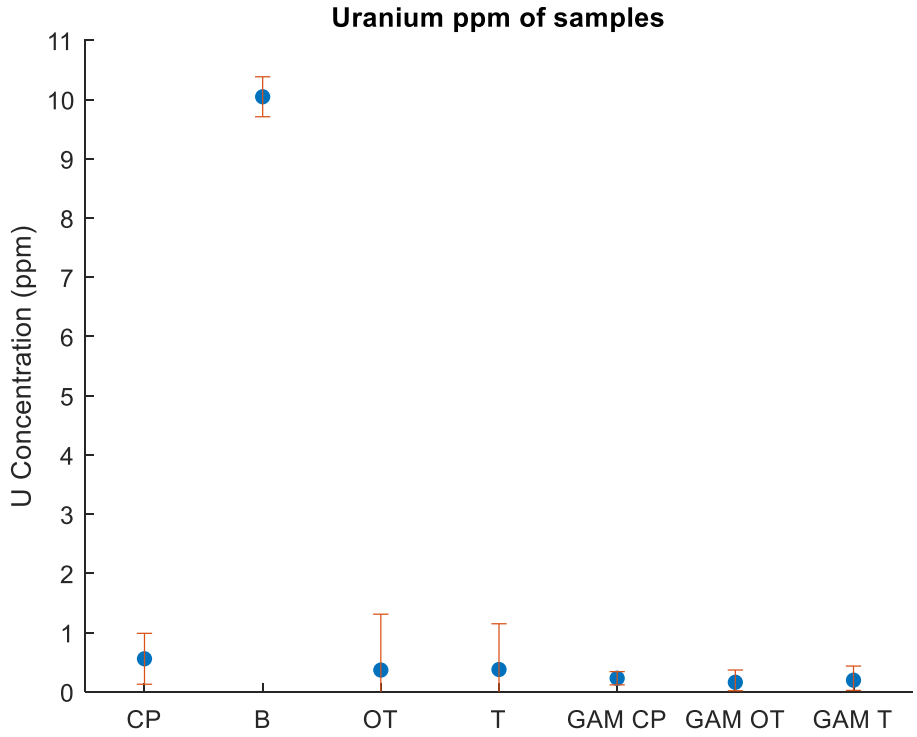

Figure 9: Concentration of uranium in the samples (excluding sample UITE due to its high abundance) analysed by ICP-MS/MS, with the inclusion of the calculated concentration data obtained from the GS data.

As no GS data was obtained for ^{235}U from sample B, no calculations could be performed for this sample. In contrast, sample B yielded the greatest uranium concentration of all Maralinga soil samples analysed via ICP-MS/MS. Hence, we speculate the above-mentioned absence of the ^{235}U readings in GS analysis of this sample is likely due to a human error or some other unconstrained analytical issues. As overall, all other calculated GS based concentrations were lower than those determined

independently via solution ICP-MS/MS from bulk acid digested sample. This systematic offset or discrepancy between methods (GS and ICP-MS/MS can be attributed to the energy lost as the emitted gamma rays pass through the soil sample, but this interpretation needs to be validated and confirmed by future studies and similar comparative measurements.

Cross plotting the data obtained from these calculations for samples CP, OT & T is shown in Figure 10. A rough trendline can be plotted for the 3 datapoints showing that the ICP-MS/MS data systematically yielded higher uranium concentrations (compared to GS data), but the error bars associated with each technique are too large to provide conclusive validation of such systematic difference from the unity between the two techniques.

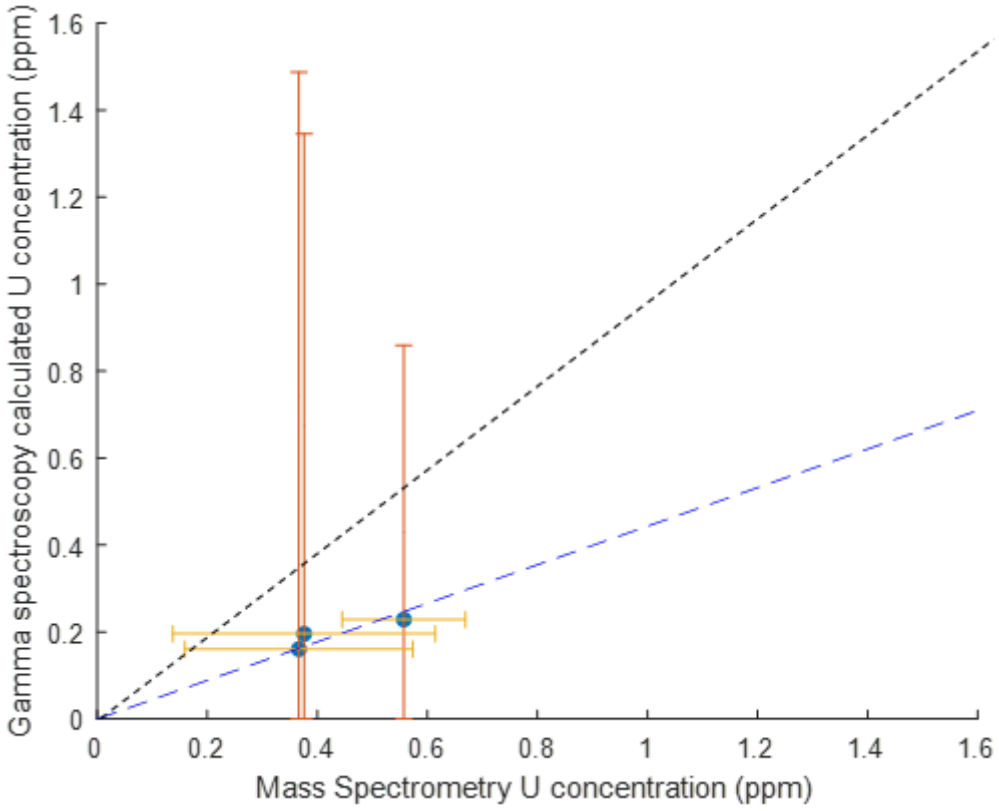

Figure 10: A cross plot of the measured and calculated uranium concentration in ppm from the GS against the concentration obtained from the ICP-MS/MS. With the trendline in blue having an equation of y = 0.278x + 0.0746 and the reference line plotted in black.

Table 5 highlights the difference in total uranium levels between samples CP and UITE, as well as the estimated range of UITE being 19.5% or 21.3% based on the technique used. Any notable use of uranium from testing would likely result in samples OT and B having a greater concentration than sample CP, however, this cannot be seen as all samples have approximately natural concentration levels from both ICP-MS and GS. The increased concentration of uranium could be absent because of the mobility of uranium during rare rainfall events. The carbonate soils at Maralinga provide an oxidizing environment, where uranium can be dissolved in water and penetrate deeper into the ground (Alloway, 2013; Cumberland et al., 2016). As only surface samples were collected this conclusion cannot be supported.

	ICP-MS obtained (ppm)	Gamma Spec Calculated (ppm)	Uranium Range (ppm)
UITE	212996 ± 551	194620 ± 22856	195,000 - 213,000
CP	0.6 ± 0.43	0.23 ± 0.11	0.2 - 0.6

Table 5: The uranium concentrations and ranges obtained for both natural samples CP and UITE using the direct measurement through ICP-MS/MS and indirectly through GS.

5.2 Uranium isotope ratio as a proxy of nuclear contamination

5.2.1 ISOTOPIC RATIOS OF STANDARDS

Isotopic data obtained from the solution ICP-MS/MS (experiment 2) resulted in a systematic shift of all results (i.e., isotopic ratios) to have a depletion in ^{235}U (relative to ^{238}U) when bracketing with the standard CRM 145 (i.e., the 'natural' uranium isotope standard). Standards supplied by Macquarie University had unknown concentrations and thus during the second test CRM U500 and CRM 145 were initially tested using the less precise 'analog' mode on ICP MS/MS instrument (Agilent 8900). The use of the SSB approach (using both standards: CRM 145 and U010) did not eliminate this systematic isotope shift as the samples we expected to be natural, CP and B, both yielded lower $^{235}U/^{238}U$ ratios relative to the expected 'natural' ratio, with CP having a value of 0.00684 ± 0.000072 where it was expected to have a 'natural' isotopic ratio similar to CRM 145's certified value of 0.00725 ± 0.000004.

The additional standards CRM U500 and CRM U010 also were affected by this shift as they differed from their known and certified isotope values. Importantly, measurements of the U500 standard gave the greatest accuracy to its known $^{235}U/^{238}$ isotope ratio; however, all other values, from remaining standards, remained discordant when corrected, suggesting that the cause was possibly a detection issue regarding ^{235}U. Finally, the standard CRM U0002 (i.e., depleted uranium reference material) could not be used to detect an accurate $^{235}U/^{238}U$ isotope ratio as the measured ^{235}U counts were extremely low. After initial correction the measured ratio for this standard was 288% greater than its certified value, whereas U010 and U500 were 0.1% and 14.5% lower than their certified values. Hence, from these findings and above test and observations,

only the CRM U500 and CRM U010 standards were used to bracket and correct the measured concentration results from the studied samples (acquired in the final run). The results from the second experiment were discarded, and the systematic shift was no longer present in the 3rd run, with both standards matching their isotopic reference values for the $^{235}U/^{238}U$ ratios.

5.2.2 VARIABILITY OF URANIUM ISOTOPE ABUNDANCES ($^{235}U/^{238}U$ RATIOS)

There was extreme variability in the uncertainties for the $^{235}U/^{238}U$ isotope ratio for measured samples due to the variable sizes of ^{235}U ion beam intensity (counts of ^{235}U) received and detected by the single collector of ICP-MS/MS. The detection of ^{235}U by GS had the greatest variability with sample UITE, as the powder was slightly coarser and harder to compact and homogenise resulting in small air pockets present throughout the sample. This resulted in a more staggered reading as radon gas built up preferentially in these air pockets and influenced the homogeneity of the sample and, in part the gamma rays emitted. The high concentration of gamma radiation emitted by the ^{235}U in sample UITE partially overwhelmed the detector, making this measurement less precise.

5.2.3 QUASI-NATURAL URANIUM ISOTOPE ABUNDANCES

All samples tested and analysed yielded a close-to-natural or 'quasi-natural' $^{235}U/^{238}U$ isotope ratio with no anomalous ^{235}U enrichment detectable within the analytical uncertainty of our approach by ICP-MS/MS. The confirmed presence of nuclear fission radionuclides measured via GS as well as evidence of 'Hot' particles from SEM-EDS analysis, confirm that the Maralinga soils contain some degree of nuclear contaminants. Previous literature from Chernobyl site identified 'non-natural' and enriched $^{235}U/^{238}U$

ratios between 0.00764 and 0.00968 (Boulyga & Becker, 2002). Fallout at the Chernobyl reactor contaminated surrounding soils with ~2% ^{235}U enriched uranium that was used as nuclear fuel. Uranium of significantly higher ^{235}U enrichment would be the required for major weapons tests which have occurred at the Maralinga site locations B and OT.

All major Maralinga sites were exposed to fission experiments and would have received contamination from either enriched uranium and/or plutonium during the testing period, based on the material(s) used in the tested weapon. Site T, which served as the testing location for the ^{239}Pu core "Pixie" design, should present a quasi-natural uranium isotope ratio due the absence of enriched uranium in the design. Sites B and OT were expected to possess detectable ^{235}Um enrichment based on their ^{235}U/^{239}Pu mixed cores. As the ^{235}U/^{238}U ratio remains quasi-natural across all samples, the contamination introduced from the nuclear testing likely only represents a small portion of the total uranium and is not above 'natural' background (i.e. natural uranium present in soils/ rocks).

The low concentration of contaminated uranium in soils is likely a result of the distance from the detonation site and thus has become diluted with natural uranium that was pre-existing. Detonation distance cannot be explored or discussed further in this study due to lack of precise location data for the analysed legacy samples. In addition, historical data also found no significant ^{235}U enrichment in soils during the radiological survey performed by TAG (MRTAC, 2003). As the three Maralinga samples had no detectable traces of artificially altered ^{235}U/^{238}U ratios, further testing would be required to refute

or confirm the technique. Performing a grid-based sampling survey of known site plumes would test the effectiveness of this technique, coupled with a more precise multi collector ICP-MS or thermal ionic mass spectrometry (TIMS) analysis of such samples for uranium isotope abundances and high precision $^{235}U/^{238}U$ isotope ratios.

5.3 Measured man-made radionuclide contamination

As previously shown in Figure 2 and Figure 3, ^{137}Cs and ^{152}Eu isotopes are considered radioactive products of fission of ^{235}U, while ^{241}Am is produced through the fission of ^{239}Pu. The measured gamma radiation of these man-made radionuclides assists in providing insight into the sources of nuclear contamination found at each site. The ^{137}Cs and ^{152}Eu present in all Maralinga samples including the sample T which should only have been exposed to ^{241}Am. Contamination of ^{137}Cs was below 0.05 Bq/g and ^{152}Eu fell below 0.15 Bq/g. However, the contamination of these nuclides in soil samples OT and B is much greater, due to the larger "Red Beard" design that was used in these tests, as displayed in Figures 8C-E. ^{241}Am was detected in all Maralinga samples except sample B. The lack of ^{241}Am indicates that there was no ^{239}Pu that underwent fission, which contradicts historical statements that a "Red Beard" was tested at site B. This discrepancy associated with the sample B is also linked the observed absence of ^{235}U, as previously mentioned, and is likely due to a misinterpretation of the gamma ray absorption spectrum or some other yet unconstrained factors.

As expected, both natural sourced uranium samples, CP and UITE, contained no detectable levels of the radionuclides ^{137}Cs, ^{152}Eu and ^{241}Am. This supports that samples T, OT & B are affected by the man-made radionuclide deposition after the major fission experiments at Maralinga, while samples CP and UITE are contamination free. Sample

CP contains detectable ^{235}U at similar levels to samples T and OT. The average concentration of uranium within analysed soils is commonly 2ppm with all samples falling within the expected natural concentrations of for rural SA soil ranging from 0.23 to 40 ppm (IAEA., 2022: Hill et al., 2020).

Interestingly, there is no detectable difference in gamma radiation data (or ICP MS/MS data) for ^{235}U abundance sourced from purported nuclear contamination and/or that from natural background. Due to variability in concentration of naturally sourced uranium and low levels of nuclear sourced U source, this study was not able to identify and detect such artificially introduced and man-made ^{235}U enrichment through analytical approaches and techniques applied in this study. However, as the artificially introduced ^{235}U is in disequilibria with its daughter products, the initial ^{235}U present in the sample(s) could be calculated using the original daughter products found within the soil if detectable. Nuclear uranium ^{235}U contamination has yet to reach equilibria with its daughter products due to its long half-life so the measurable difference could be identified.

6. CONCLUSIONS

The use of $^{235}U/^{238}U$ isotope ratios as a tracer for possible man-made U contamination linked to the nuclear tests and trails performed in Maralinga, SA, have showed close to natural (quasi-natural) U isotope abundances in local soils across all studied samples and sites. Thus, expected enrichment in ^{235}U from nuclear test was not present or detected within a 0.14 % error margin of our ICP MS/MS method, indicating that the concentration of nuclear-sourced U within the sampled Maralinga soils was diluted or swamped by comparatively greater levels of natural U present in the soils. Also, the identified uranium-rich (U_3O_8) 'hot' particles found within some soils showed no sign of plutonium (Pu) enrichment or inhomogeneity (unlike reported in previous literature) indicating that these particles might be perhaps also natural uranium-rich grains. However, other man-made radionuclides identified in the studied Maralinga soils through gamma spectroscopy, such as ^{137}Cs, ^{152}Eu and ^{241}Am, confirm the presence of nuclear fission contamination within the soils, which in turn provide greater insight into the source of the nuclear material used. Further investigation could be undertaken to isolate the natural uranium present based on its daughter products against the artificially introduced uranium ^{235}U, which is in disequilibria with its decay chain; and future high precision $^{235}U/^{238}U$ isotope measurements via multi-collector ICP MS or TIMS can further confirm and quantify the levels of enriched U in the Maralinga soils.

7. ACKNOWLEDGMENTS

Thank you so much to my supervisor Juraj Farkas & my Co supervisors Tony Hooker & Nigel Spooner. Additional thanks to Lucy McGee & Simon Turner for their help regarding procuring the additional standards used in this project. The assistance of Jarrah Mik, Chris Kalnins, Joseph Builth-Williams & Robert Klaebe for their assistance & knowledge regarding laboratory processes was invaluable. Dr Sarah Gilbert & Aofie Mcfadden at Adelaide microscopy for their assistance in ICP-MS & SEM. And finally, Katie Howard & Derrick Hasterok for their assistance throughout the year.

8. REFERENCES

Alloway, B. J. (2013). Uranium. In B. J. Alloway (Ed.), *Heavy Metals in Soils: Trace Metals and Metalloids in Soils and their Bioavailability* (pp. 565-577). Springer Netherlands. https://doi.org/10.1007/978-94-007-4470-7_26

Archive, N. W. (2007). *Britain's Nuclear Weapons*. Retrieved 17/10/22 from https://nuclearweaponarchive.org/Uk/UKTesting.html

Boulyga, S. F., & Becker, J. S. (2002). Isotopic analysis of uranium and plutonium using ICP-MS and estimation of burn-up of spent uranium in contaminated environmental samples. *J. Anal. At. Spectrom.*, *17*(9), 1143-1147. https://doi.org/10.1039/b202196j

Browne, E. (2003). *Nucl. Data Sheets*, *98*, 688. https://www.scopus.com/inward/record.uri?eid=2-s2.0-4544255235&partnerID=40&md5=91b0ee6e7b6cb5aa765b609e748dfe52

Browne, E., & Tuli, J. K. (2007). Nuclear Data Sheets for A = 137. *Nuclear Data Sheets*, *108*(10), 2173-2318. https://doi.org/https://doi.org/10.1016/j.nds.2007.09.002

Cook, M., Etschmann, B., Ram, R., Ignatyev, K., Gervinskas, G., Conradson, S. D., Cumberland, S., Wong, V. N. L., & Brugger, J. (2021). The nature of Pu-bearing particles from the Maralinga nuclear testing site, Australia. *Sci Rep*, *11*(1), 10698. https://doi.org/10.1038/s41598-021-89757-5

Cooper, M. B., Burns, P. A., Tracy, B. L., Wilks, M. J., & Williams, G. A. (1994). Characterization of plutonium contamination at the former nuclear weapons testing range, at Maralinga in South Australia. *Journal of Radioanalytical and Nuclear Chemistry*, *177*(1), 161-184. https://doi.org/10.1007/BF02132420

Cumberland, S., Douglas, G., Grice, K., & Moreau, J. (2016). Uranium mobility in organic matter-rich sediments: A review of geological and geochemical processes. *Earth-Science Reviews*, *159*. https://doi.org/10.1016/j.earscirev.2016.05.010

Goldstein, S. J., Price, A. A., Hinrichs, K. A., Lamont, S. P., Nunn, A. J., Amato, R. S., Cardon, A. M., & Gurganus, D. W. (2021). High-precision measurement of U-Pu-Np-Am concentrations and isotope ratios in environmental reference materials by mass spectrometry. *J Environ Radioact*, *237*, 106689. https://doi.org/10.1016/j.jenvrad.2021.106689

Hill, S. M., Hore, S. B., & Normington, V. J. (2020). Uranium in animals, vegetables and minerals: landscape geochemical and biogeochemical expressions of the Four Mile West sedimentary uranium deposit, South Australia. *Australian Journal of Earth Sciences*, *67*(8), 1161-1194. https://doi.org/10.1080/08120099.2020.1812717

IAEA (2022). *Depleted Uranium*. Retrieved 18/10/22 from https://www.iaea.org/topics/spent-fuel-management/depleted-uraniumium

Ikeda-Ohno, A., Shahin, L. M., Howard, D. L., Collins, R. N., Payne, T. E., & Johansen, M. P. (2016). Fate of Plutonium at a Former Nuclear Testing Site in Australia. *Environmental Science & Technology*, *50*(17), 9098-9104. https://doi.org/10.1021/acs.est.6b01864

James, J. M. (1988). Tietkens Plain Karst - Maralinga. *Australian Radiation Laboratory*.

Johansen, M. P., Child, D. P., Davis, E., Doering, C., Harrison, J. J., Hotchkis, M. A., Payne, T. E., Thiruvoth, S., Twining, J. R., & Wood, M. D. (2014). Plutonium in wildlife and soils at the Maralinga legacy site: persistence over decadal time scales. *J Environ Radioact*, *131*, 72-80. https://doi.org/10.1016/j.jenvrad.2013.10.014

Kaspar, T. C., Lavender, C. A., & Dibert, M. W. *Evaluation of Uranium-235 Measurement Techniques*. United States. https://doi.org/10.2172/1408200

Lal, R., Fifield, L. K., Tims, S., & Wasson, R. (2017). 239 Pu fallout across continental Australia: Implications on 239 Pu use as a soil tracer. *Journal of Environmental Radioactivity*, *178-179*. https://doi.org/10.1016/j.jenvrad.2017.08.009

Loebe, T., Hettwig, B., & Fischer, H. W. (2014). Detection of long-lived europium-152 in samarium-153-lexidronam. *Applied radiation and isotopes : including data, instrumentation and methods for use in agriculture, industry and medicine*, *94*, 40–43.

Lokan, K. H. (1985). Residual Radioactive Contamination at Maralinga and EMU, 1985. *Australian Radiation Laboratory*.

Lorna Arnold, M. S. (2006). *Britain, Australia and the Bomb (The Nuclear Tests and their Aftermath)* (Vol. 1). Palgrave Macmillan London. https://doi.org/https://doi.org/10.1057/9780230627338

Mathew, K. J., O'Connor, G., Hasozbek, A., & Kraiem, M. (2013). Total evaporation method for uranium isotope-amount ratio measurements. *Journal of Analytical Atomic Spectrometry*, *28*(6). https://doi.org/10.1039/c2ja30321c

MRTAC. (2003). *Rehabilitation of former nuclear test sites at Emu and Maralinga (Australia) 2003* (0642 77328 9). J. S. M. P. Group.

Neuhoff, J. (1987). *Certificate of Analysis CRM U0002* https://science.osti.gov/-/media/nbl/pdf/price-lists/certificates/CRM_U0002_1_Gram_Sample_Size_March_2008.pdf

Neuhoff, J. (2008a). *Certificate of Analysis CRM U010* https://science.osti.gov/-/media/nbl/pdf/price-lists/certificates/CRM_U0002_1_Gram_Sample_Size_March_2008.pdf

Neuhoff, J. (2008b). *Certificate of Analysis CRM U500* https://science.osti.gov/-/media/nbl/pdf/price-lists/certificates/CRM_U0002_1_Gram_Sample_Size_March_2008.pdf
Neuhoff, J. (2010). *Certificate of Analysis CRM 145* https://science.osti.gov/-/media/nbl/pdf/price-lists/certificates/CRM_U0002_1_Gram_Sample_Size_March_2008.pdf
Nuclear, W. (2022). *Uranium Enrichment.* https://world-nuclear.org/information-library/nuclear-fuel-cycle/conversion-enrichment-and-fabrication/uranium-enrichment.aspx#:~:text=Most%20reactors%20are%20light%20water,%2Denriched%20uranium%20(LEU).
Oliver, I. W., Graham, M. C., MacKenzie, A. B., Ellam, R. M., & Farmer, J. G. (2008). Depleted Uranium Mobility Across a Weapons Testing Site: Isotopic Investigation of Porewater, Earthworms, and Soils. *Environmental Science & Technology*, *42*(24), 9158-9164. https://doi.org/10.1021/es8013634
Parkinson, A. (2004). The Maralinga rehabilitation project: final report. *Medicine, Conflict and Survival*, *20*(1), 70-80. https://doi.org/10.1080/13623690412331302304
Peter N. Johnston, P. A. B., Malcom B. Cooper & Geoffrey A. Williams. (1988). Isotopic Ratios of Actinides Used in British Nuclear Trials at Maralinga and Emu. *Australian Radiation Laboratory*.
SRP. (2022). *Human Health Fact sheet*. Health Physics Society. http://hpschapters.org/northcarolina/NSDS/cobalt.pdf
Thangam, V., Rajalakshmi, A., Chandrasekaran, A., & Jananee, B. (2022). Measurement of natural radioactivity in river sediments of Thamirabarani, Tamilnadu, India using gamma ray spectroscopic technique. *International Journal of Environmental Analytical Chemistry*, *102*(2), 422-433. https://doi.org/10.1080/03067319.2020.1722815
Tims, S. G., Froehlich, M. B., Fifield, L. K., Wallner, A., & De Cesare, M. (2016). 236U and 239,240Pu ratios from soils around an Australian nuclear weapons test site. *Journal of Environmental Radioactivity*, *151*, 563-567. https://doi.org/https://doi.org/10.1016/j.jenvrad.2015.06.020
Schofield, A 1985, *Listing of minor trials (unclassified)*, submission to the Royal Commission into British Nuclear Tests in Australia (RC 350), 28 February 1985.
Stewart, K 1960, *Vixen A Trials*, AWRE Report No. T-15/60, United Kingdom Atomic Energy Authority.
UAB. (2007). Radiation Safety Procedures Manual Ninth Edition, 2007. The University of Alabama at Birmingham.
WISE Uranium (2018, October 19) Unit Converer. Retrieved 17/10/22 from https://www.wise-uranium.org/cunit.html

APPENDICES

Appendix A: SEM Absorption Spectra with characterised elements

Breakaway

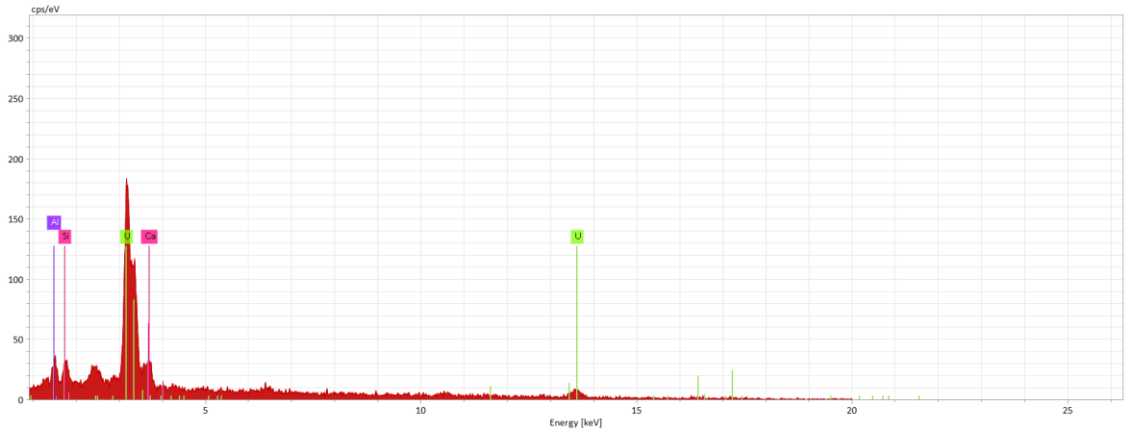

Tadje

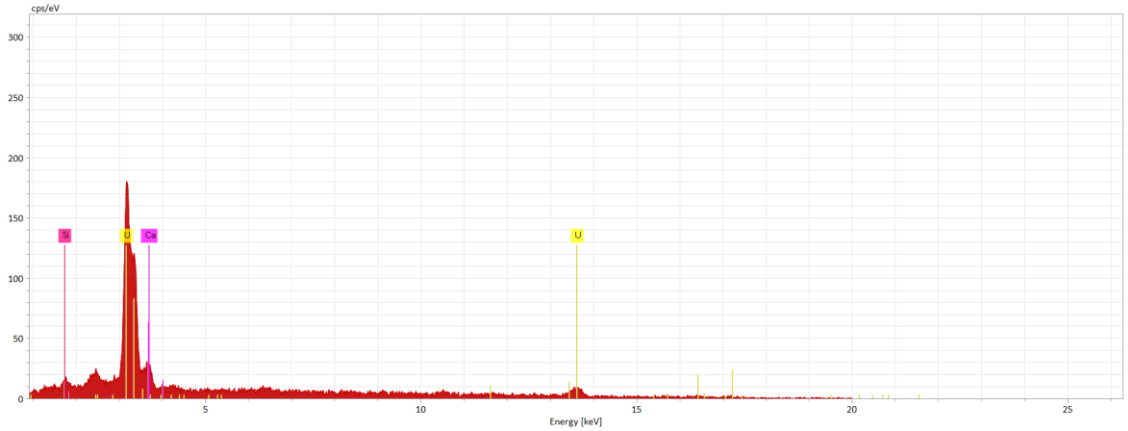

Appendix B: Mixed A Standard concentration curve & CPS/RSD curve for ^{238}U

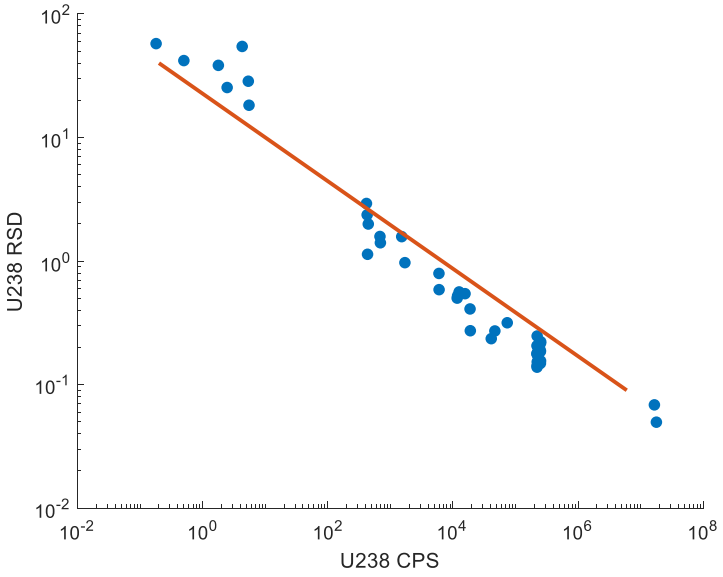

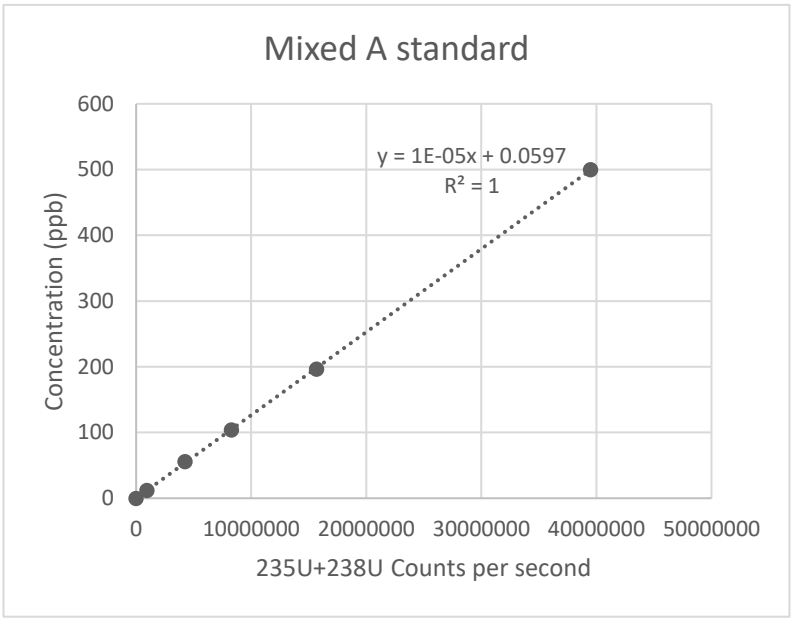

Appendix C: Sample digestion methodology

(Provided by Dr Robert Klaebe)

Stage 1: 28M (48%) HF DIGESTION (Allow 55 h to complete)
CAUTION: EXTREMELY HAZARDOUS HYDROFLUORIC ACID

All staff and students must have received prior safety training on how to use HF for the digestion of samples before you commence this stage. HF must only be dispensed in the fume cupboard and requires the following PPE. plastic apron, gloves, sleeve protectors and face shield. LOWER THE FUME CUPBOARD SASH AS LOW AS PRACTICABLE TO AVOID FUMES OR SPLASHES.

1. Add 4ml 28M HF, cap the container then place on a hotplate at 140°C. Label the equipment with the signage card and heat for 48 h.

2. Allow to cool, then gently tap the vial (at a slight angle) to collect any acid drops from the top or sides to the bottom.

3. Uncap the vial and evaporate till almost dry at 140°C. (Usually 2-4h depending on vial used) This removes silicon as silicon tetrafluoride (SiF4), but insoluble fluorides can also form as the sample is dried in the presence of excess HF. To reduce the likelihood of insoluble fluorides, nitric acid dilution is used (Stage 2).

Stage 2: 7M HNO3 DILUTION (Allow 2-3 h to complete)

4. Add 1mL sd ~ 7M HNO3 just before the sample dries and allow to evaporate to dryness at 140°C. (and maybe repeat it.).

5. After the sample has dried add ~ 2mL sd ~ 7M HNO3.

6. Remove from the hotplate and allow to cool.

Stage 3:28M (48%) HF DIGESTION (Allow 55 h to complete)

7. Add 4mL sd 28M HF from the dispenser.

8. Recap and heat for a further 48 hours at 140°C on a hot plate.

9. Allow to cool, then gently tap the vial (at a slight angle) to collect any acid drops from the top or sides to the bottom.

10. Uncap vial and evaporate to dryness at 140°C. (Usually takes 2-4 h depending on vial) like in stage 2 This removes silicon as SiF4 to reduce the likelihood of insoluble fluorides forming, nitric acid dilution is used (Stage 4).

Stage 4: 7M HNO3 DILUTION (Allow 2-3 h to complete)

11. Add 1mL sd~ 7M HNO3 just before the sample dries and allow to evaporate to dryness at 140°C. (and maybe repeat it.). Label the equipment with the signage card.

Stage 5: 6M HCI DIGESTION (Allow 3-12h to complete)

12. Remove from the hotplate and allow to cool.

13. After the sample has cooled add 6mL sd ~ 6M HCI to the solid residue.

14. Recap then return vial to the hot plate at 140°C until completely dissolved (several hours to overnight). Label the equipment with the signage card.

15. Allow to cool then uncap and heat on the hot plate set at 140°C until dry. Y Note: Centrifuge procedure can be started whilst this is evaporating to dryness.

Appendix D: GS results

Uraninite

Nuclide Name	MDA (Bq /unit)	Decision Level (Bq /unit)	Confidence Int low (Bq /unit)	Confidence Int up (Bq /unit)	Wt. mean Activity (Bq /unit)	Wt. Mean Act Unc (Bq /unit)	Best Est Activity (Bq /unit)	Best Est Act Unc (Bq /unit)
K-40	-	-	-	-	-	-	-	-
Cs-137	-	-	-	-	-	-	-	-
Eu-152	-	-	-	-	-	-	-	-
TL-208	-	-	-	-	-	-	-	-
Pb-210	7.20E+02	3.39E+02	2.98E+03	5.54E+03	4.26E+03	6.52E+02	4.26E+03	6.52E+02
PB-212	-	-	-	-	-	-	-	-
BI-214	2.04E+02	1.01E+02	6.32E+04	6.99E+04	6.66E+04	1.72E+03	6.66E+04	1.72E+03
PB-214	1.89E+02	9.29E+01	6.71E+04	8.36E+04	7.54E+04	4.22E+03	7.54E+04	4.22E+03
TH-227	3.43E+02	1.42E+02	1.63E+03	3.19E+03	2.41E+03	4.00E+02	2.41E+03	4.00E+02
AC-228	-	-	-	-	-	-	-	-
TH-230	6.45E+03	3.08E+03	6.96E+03	1.64E+04	1.17E+04	2.41E+03	1.17E+04	2.41E+03
PA-231	1.54E+03	6.63E+02	1.76E+01	2.95E+02	1.37E+02	7.95E+01	1.45E+02	7.24E+01
Pa-234m	1.24E+04	6.16E+03	1.13E+05	1.38E+05	1.26E+05	6.59E+03	1.26E+05	6.59E+03
TH-234	7.64E+02	3.12E+02	4.28E+03	1.32E+04	8.75E+03	2.28E+03	8.75E+03	2.28E+03
U-235	5.55E+01	2.71E+01	1.36E+03	1.74E+03	1.55E+03	9.66E+01	1.55E+03	9.66E+01
AM-241	-	-	-	-	-	-	-	-

Coober Pedy

	MDA (Bq /unit)	Decision Level (Bq /unit)	Confidence Int low (Bq /unit)	Confidence Int up (Bq /unit)	Wt. mean Activity (Bq /unit)	Wt. Mean Act Unc (Bq /unit)	Best Est Activity (Bq /unit)	Best Est Act Unc (Bq /unit)
K-40	5.48E-02	2.72E-02	1.97E-01	2.74E-01	2.36E-01	1.97E-02	2.36E-01	1.97E-02
Cs-137	-	-	-	-	-	-	-	-
Eu-152	-	-	-	-	-	-	-	-
TL-208	2.82E-03	1.39E-03	7.34E-03	1.12E-02	9.28E-03	9.92E-04	9.28E-03	9.92E-04
Pb-210	1.82E-02	8.55E-03	2.86E-02	6.13E-02	4.50E-02	8.34E-03	4.50E-02	8.34E-03
PB-212	2.08E-03	1.02E-03	2.99E-02	4.21E-02	3.60E-02	3.11E-03	3.60E-02	3.11E-03
BI-214	7.17E-03	3.54E-03	6.17E-02	7.82E-02	6.99E-02	4.22E-03	6.99E-02	4.22E-03
PB-214	4.79E-03	2.35E-03	1.16E-02	1.74E-02	1.45E-02	1.46E-03	1.45E-02	1.46E-03
TH-227	-	-	-	-	-	-	-	-
AC-228	1.44E-02	7.13E-03	2.29E-02	2.98E-02	2.64E-02	1.77E-03	2.64E-02	1.77E-03
TH-230	-	-	-	-	-	-	-	-
PA-231	-	-	-	-	-	-	-	-
Pa-234m	4.44E-01	2.20E-01	7.62E-01	1.32E+00	1.04E+00	1.43E-01	1.04E+00	1.43E-01
TH-234	1.57E-02	6.37E-03	4.97E-03	2.71E-02	1.59E-02	5.70E-03	1.59E-02	5.63E-03
U-235	1.42E-03	6.94E-04	9.29E-04	2.71E-03	1.82E-03	4.55E-04	1.82E-03	4.55E-04
AM-241	-	-	-	-	-	-	-	-

Tadje

	MDA (Bq /unit)	Decision Level (Bq /unit)	Confidence Int low (Bq /unit)	Confidence Int up (Bq /unit)	Wt. mean Activity (Bq /unit)	Wt. Mean Act Unc (Bq /unit)	Best Est Activity (Bq /unit)	Best Est Act Unc (Bq /unit)
K-40	1.01E-01	5.01E-02	3.81E-02	1.60E-01	9.89E-02	3.12E-02	9.90E-02	3.11E-02
Cs-137	6.69E-03	3.29E-03	6.91E-03	1.54E-02	1.11E-02	2.15E-03	1.11E-02	2.15E-03
Eu-152	5.26E-03	2.54E-03	9.92E-02	1.19E-01	1.09E-01	5.11E-03	1.09E-01	5.11E-03
TL-208	-	-	-	-	-	-	-	-
Pb-210	3.30E-02	1.54E-02	4.37E-02	8.63E-02	6.50E-02	1.09E-02	6.50E-02	1.09E-02
PB-212	4.68E-03	2.28E-03	7.28E-03	1.39E-02	1.06E-02	1.69E-03	1.06E-02	1.69E-03
BI-214	1.26E-02	6.19E-03	6.51E-02	8.70E-02	7.60E-02	5.58E-03	7.60E-02	5.58E-03
PB-214	8.38E-03	4.09E-03	8.37E-03	1.76E-02	1.30E-02	2.35E-03	1.30E-02	2.35E-03
TH-227	-	-	-	-	-	-	-	-
AC-228	-	-	-	-	-	-	-	-
TH-230	-	-	-	-	-	-	-	-
PA-231	-	-	-	-	-	-	-	-
Pa-234m	1.05E+00	5.19E-01	8.98E-01	2.18E+00	1.54E+00	3.28E-01	1.54E+00	3.28E-01
TH-234	3.16E-02	1.28E-02	6.11E-04	2.38E-02	7.40E-03	8.05E-03	9.96E-03	6.26E-03
U-235	3.18E-03	1.55E-03	1.85E-04	3.46E-03	1.56E-03	9.57E-04	1.67E-03	8.60E-04
AM-241	3.97E-03	1.92E-03	1.81E-01	2.72E-01	2.27E-01	2.32E-02	2.27E-01	2.32E-02

One Tree

	MDA (Bq /unit)	Decision Level (Bq /unit)	Confidence Int low (Bq /unit)	Confidence Int up (Bq /unit)	Wt. mean Activity (Bq /unit)	Wt. Mean Act Unc (Bq /unit)	Best Est Activity (Bq /unit)	Best Est Act Unc (Bq /unit)
K-40	7.50E-02	3.72E-02	1.52E-01	2.17E-01	1.84E-01	1.66E-02	1.84E-01	1.66E-02
Cs-137	7.14E-03	3.52E-03	2.09E+00	2.65E+00	2.37E+00	1.42E-01	2.37E+00	1.42E-01
Eu-152	3.79E-03	1.84E-03	1.63E+00	1.78E+00	1.70E+00	3.79E-02	1.70E+00	3.79E-02
TL-208	4.56E-03	2.25E-03	3.70E-03	6.85E-03	5.27E-03	8.06E-04	5.27E-03	8.06E-04
Pb-210	5.05E-02	2.38E-02	5.90E-01	1.05E+00	8.20E-01	1.17E-01	8.20E-01	1.17E-01
PB-212	4.04E-03	1.97E-03	1.44E-02	2.09E-02	1.77E-02	1.65E-03	1.77E-02	1.65E-03
BI-214	1.08E-02	5.35E-03	9.71E-02	1.22E-01	1.09E-01	6.26E-03	1.09E-01	6.26E-03
PB-214	8.04E-03	3.95E-03	1.85E-02	2.86E-02	2.36E-02	2.57E-03	2.36E-02	2.57E-03
TH-227	-	-	-	-	-	-	-	-
AC-228	-	-	-	-	-	-	-	-
TH-230	-	-	-	-	-	-	-	-
PA-231	-	-	-	-	-	-	-	-
Pa-234m	8.41E-01	4.17E-01	1.97E+00	2.60E+00	2.28E+00	1.62E-01	2.28E+00	1.62E-01
TH-234	3.48E-02	1.42E-02	4.50E-04	2.32E-02	4.91E-03	8.72E-03	9.07E-03	6.18E-03
U-235	2.77E-03	1.35E-03	1.41E-04	2.93E-03	1.28E-03	8.31E-04	1.39E-03	7.36E-04
AM-241	4.48E-03	2.17E-03	8.25E-01	1.24E+00	1.03E+00	1.05E-01	1.03E+00	1.05E-01

Breakaway

	MDA (Bq /unit)	Decision Level (Bq /unit)	Confidence Int low (Bq /unit)	Confidence Int up (Bq /unit)	Wt. mean Activity (Bq /unit)	Wt. Mean Act Unc (Bq /unit)	Best Est Activity (Bq /unit)	Best Est Act Unc (Bq /unit)
K-40	1.01E-01	5.00E-02	1.54E-01	2.34E-01	1.94E-01	2.05E-02	1.94E-01	2.05E-02
Cs-137	9.34E-03	4.61E-03	6.18E-01	7.84E-01	7.01E-01	4.23E-02	7.01E-01	4.23E-02
Eu-152	4.89E-03	2.37E-03	1.66E+00	1.81E+00	1.74E+00	3.91E-02	1.74E+00	3.91E-02
TL-208	5.29E-03	2.60E-03	4.71E-04	4.09E-03	2.21E-03	9.62E-04	2.23E-03	9.29E-04
Pb-210	5.99E-02	2.82E-02	6.13E-01	1.09E+00	8.52E-01	1.22E-01	8.52E-01	1.22E-01
PB-212	5.11E-03	2.49E-03	1.24E-02	1.84E-02	1.54E-02	1.55E-03	1.54E-02	1.55E-03
BI-214	1.40E-02	6.91E-03	1.45E-01	1.81E-01	1.63E-01	9.20E-03	1.63E-01	9.20E-03
PB-214	8.63E-03	4.23E-03	1.73E-02	2.51E-02	2.12E-02	1.99E-03	2.12E-02	1.99E-03
TH-227	-	-	-	-	-	-	-	-
AC-228	-	-	-	-	-	-	-	-
TH-230	-	-	-	-	-	-	-	-
PA-231	-	-	-	-	-	-	-	-
Pa-234m	1.15E+00	5.71E-01	2.06E+00	2.88E+00	2.47E+00	2.08E-01	2.47E+00	2.08E-01
TH-234	5.22E-03	2.53E-03	3.92E-01	5.88E-01	4.90E-01	4.99E-02	4.90E-01	4.99E-02
U-235	-	-	-	-	-	-	-	-
AM-241	-	-	-	-	-	-	-	-

Appendix E: CPS results from experiment 3

Sample	238 -> 238 U [He]	238 -> 238 / 235 -> 235 U [He]
Mixed_A_10ppb	834759	1707
Mixed_A_100ppb	5803152	15603
Mixed_A_500ppb	27388582	73747
CRM500_10	257028	252694
CRM500_10	255799	251213
CRM500_10	255871	251437
CRM500_10	254720	250122
CRM500_10	255371	250714
U010_10	1892483	18771
U010_10	1915968	18952
CRM500_10	252574	247650
CP1	97602	692
CP2	96229	681
CRM500_10	247856	243138
OT1	62288	443
OT2	58226	415
CRM500_10	239533	234681
B1	1675369	11876
B2	1652394	11683
CRM500_10	234659	229911
T1	60765	431
T2	59308	425
CRM500_10	230032	225458
UITE1	843100	5974
UITE2	845591	6003
CRM500_10	227783	223168
10ppb	740544	1518
100ppb	4792862	12567
U500#	14664826	17862798
U500	13630432	16599750
CRM500_10	229675	225039
CRM145#	5135505	46771
CRM145	4502497	40950
CRM500_10	227692	223226